Performance of Tantalum-Tungsten Alloy Selective Emitters in Thermophotovoltaic Systems

Veronika Stelmakh[a] and Veronika Rinnerbauer[b] and Walker R. Chan[a] and Jay J. Senkevich[a] and John D. Joannopoulos[a] and Marin Soljačić[a] and Ivan Celanovic[a]

[a]Institute for Soldier Nanotechnology, Massachusetts Institute of Technology, Cambridge, Massachusetts, USA;
[b]Johannes Kepler University Linz, Institute of Semiconductor and Solid State Physics, Altenbergerstr. 69 4040 Linz, Austria

ABSTRACT

A tantalum tungsten solid solution alloy, Ta 3% W, based 2D photonic crystal (PhC) was designed and fabricated for high-temperature energy conversion applications. Ta 3% W presents advantages compared to the non-alloys as it combines the better high-temperature thermomechanical properties of W with the more compliant material properties of Ta, allowing for a direct system integration path of the PhC as selective emitter/absorber into a spectrum of energy conversion systems. Indeed metallic PhCs are promising as high performance selective thermal emitters for thermophotovoltaics (TPV), solar thermal, and solar TPV applications due to the ability to tune their spectral properties and achieve highly selective emission. A 2D PhC was designed to have high spectral selectivity matched to the bandgap of a TPV cell using numerical simulations and fabricated using standard semiconductor processes. The emittance of the Ta 3% W PhC was obtained from near-normal reflectance measurements at room temperature before and after annealing at 1200°C for 24h in vacuum with a protective coating of 40 nm HfO_2, showing high selectivity in agreement with simulations. SEM images of the cross section of the PhC prepared by FIB confirm the structural stability of the PhC after anneal, i.e. the coating effectively prevented structural degradation due to surface diffusion. The mechanical and thermal stability of the substrate was characterized as well as the optical properties of the fabricated PhC. To evaluate the performance of the selective emitters, the spectral selectivity and useful emitted power density are calculated as a function of operating temperature. At 1200°C, the useful emitted irradiance is selectively increased by a factor of 3 using the selective emitter as compared to the non-structured surface. All in all, this paper demonstrates the suitability of 2D PhCs fabricated on polycrystalline Ta-W substrates with an HfO_2 coating for TPV applications.

Keywords: Thermophotovoltaics, Photonic crystals, High-temperature energy conversion, Tantalum-tungsten alloy, Spectral selectivity, Thermal barrier coating, Selective emitter/absorber.

1. INTRODUCTION

Spectrally selective emitters and absorbers are critical components of high temperature thermal-to-electrical energy conversion schemes such as thermophotovoltaic (TPV) solar thermal and solar thermophotovoltaic systems. TPV is a solid state energy conversion scheme with no moving parts and low maintenance requirements that allows for scalable energy production with high power density from a variety of energy sources. In TPV systems, thermal radiation from a heat source at high temperature drives a suitable small bandgap photovoltaic

Further author information: (Send correspondence to V.S)
V.S: E-mail: stelmakh@mit.edu, Telephone: +1 617 324 6443

Energy Harvesting and Storage: Materials, Devices, and Applications V, edited by Nibir K. Dhar, Palani Balaya, Achyut K. Dutta, Proc. of SPIE Vol. 9115, 911504 · © 2014 SPIE
CCC code: 0277-786X/14/$18 · doi: 10.1117/12.2043696

cell. The heat can be produced by hydrocarbon combustion ideal for lightweight, high power density portable power sources,[1–4] by radioisotopes such as a radioisotope general purpose heat source (GPHS) ideal for space missions and remote missions requiring power sources with long lifetimes and low maintenance,[5] or by solar radiation absorbed by a suitable absorber and converted to heat.[6] Figure 1 illustrates the principles of TPV energy conversion and the role of the spectrally selective emitter. There are three critical elements required to achieve the impressive efficiencies predicted by theoretic models for TPV energy conversion.[7] First, an efficient small bandgap PV cell is needed to convert a large spectral range of the thermal emission into electrical power. TPV cells with a bandgap at 0.68 eV (1.8 μm) for GaSb,[8] 0.62 eV (2.0 μm) for InGaAs,[9] and 0.54 eV (2.3 μm) for quaternary InGaAsSb cells,[10] are especially suitable. Second, high operating temperatures are more suitable to shift the peak of the thermal emission into the spectral range of the PV cell, preferably more than 1000°C (see Fig. 1). Third, a spectral emitter is crucial to achieve high emission in a wavelength range below the bandgap of the PV cell, as well as low emission above, to keep losses due to waste heat at a minimum.[7] Ideally, the emissivity spectrum of the selective emitter is a step function with a cutoff wavelength between high and low emissivity that is matched to the bandgap of the PV cell.

Photonic crystals are ideal as selective emitters because they offer the possibility to tailor the photonic density of states and the emissivity spectrum. Selective emitters have been realized using 1D, 2D, and 3D PhC as well as metamaterials.[11–17] Considering the high target operating temperatures, thermal stability of the microstructured surfaces and their optical properties over the long operational lifetimes plays a very important role in substrate material selection.[18] Refractory metals, such as tantalum (Ta) or tungsten (W), are advantageous due to their high melting point, low vapor pressure and low infrared emissivity. The Ta-W alloy used in this study presents critical advantages compared to non-alloys as it combines the better thermomechanical properties of W with the more compliant material properties of Ta, allowing a direct system integration path, i.e. machining and welding. In addition, at high temperatures, the mechanical stability of the selective emitters made from the Ta-W alloy is greatly enhanced in comparison to pure Ta which is beneficial for overall system stability where degradation, such as creep and deflection, can play a critical role in system failure.[19] There are several main driving factors for thermal degradation of microstructures. First, oxidation, and evaporation and redeposition are prevented

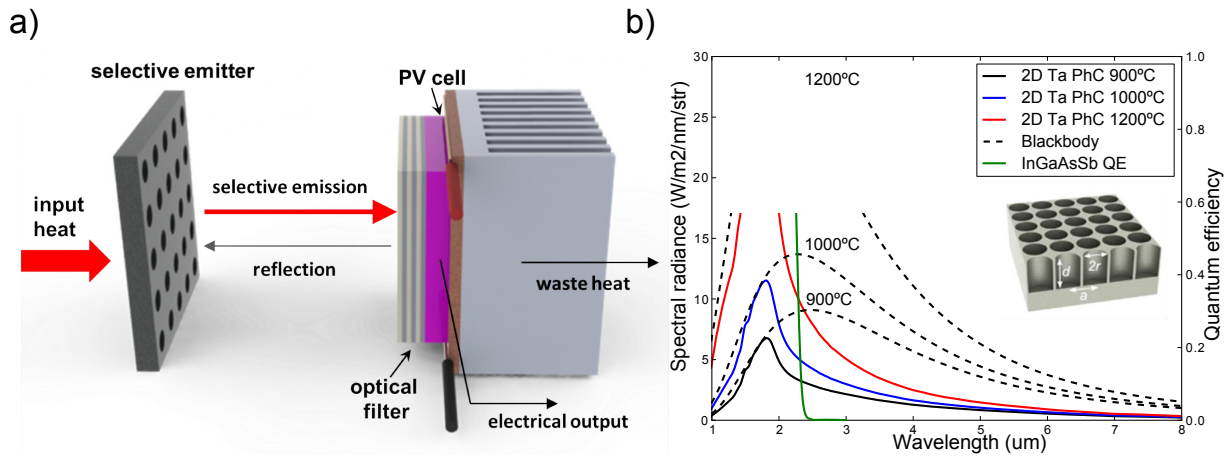

Figure 1: (Color online) (a) TPV energy conversion scheme with selective emitter, optional optical filter and PV cell. (b) Spectral emission from a Ta PhC (red) matched to the EQE of an InGaAsSb cell (green) and compared to blackbody emission at different temperatures. Inset: PhC design of a square array of cylindrical cavities.

by using refractory metals in a vacuum environment. Second, degradation by grain growth and grain diffusion in polycrystalline substrates is prevented by pre-annealing the substrates to achieve stable, large grains. Third, surface reactions and surface diffusion are the main remaining issue.[20,21]

In this paper, the performance of different PhCs was evaluated and compared to a system without a 2D PhC. At 1500K (1227°C), the useful emitted irradiance was found to be selectively increased by a factor of 3 using the selective emitter compared to the non-structured Ta surface. The spectral selectivity was found to increase by more than 10% using the selective emitter. A Ta 3% W PhC optimized for a InGaAsSb PV cell was fabricated and a thin conformal coating of HfO_2 was used as a surface protection and thermal barrier coating.[16–18] The thermal stability of the fabricated structures was tested over 24h at 1200°C without major degradation. All in all, this paper demonstrates the suitability of 2D PhCs fabricated on polycrystalline Ta 3% W substrates for high-temperature energy conversion.

2. PHOTONIC CRYSTAL DESIGN

2.1 Simulation methods

The 2D PhC consists of a square array of cylindrical cavities etched into the Ta-W substrate to selectively enhance the spectral emissivity in a certain spectral range matched to the TPV cell. In the first step, the geometrical parameters of the PhC are optimized to match the target system parameters of the system. Three PhCs were designed to match (I) a bandgap of 2.3 μm (0.54 eV, InGaAsSb), (II) a bandgap of 2.0 μm (0.62 eV, InGaAs), and (III) a bandgap of 1.8 μm (0.68 eV, GaSb). Both the hemispherical emission and the change of material parameters at high temperature are taken into account in the simulation and optimization.

The spectral emissivity ε of the 2D TaW PhC at normal incidence is determined via finite-difference time-domain (FDTD) numerical methods.[22] The material properties of the substrate are taken into account using a Lorentz-Drude model fitted to elevated temperature emissivity (1205°C) to capture the optical dispersion of the substrate at high temperature. It was verified that the measured reflectance, and therefore also emissivity, of Ta and the Ta 3% W substrate used is virtually identical. The high memory requirements and computational speed of FDTD methods however limit its application in determining the angular dependent emissivity and finding the global optimum for a TPV system. Thus, for quicker estimation, a mode matching formalism is used where the reflectance is calculated by matching the radiation fields at the boundary of free space and the cylindrical cavities via expansion of the cavity modes for shorter wavelengths, utilizing a surface area weighted impedance for longer wavelengths.[23]

For optimization, the NLopt software library for nonlinear optimization developed at MIT is used with two different optimization algorithms: Controlled Random Search (CRS) with local mutation and Multi-Level Single-Linkage (MLSL) with the geometric parameters of period, cavity radius and height as optimization parameters.[24] To take into account fabrication constraints, a minimum space of 0.1 μm between cavities was imposed and the maximum cavity height was limited to 8.0 μm. It has been verified that the most significant influence on the spectral properties in the range of interest is given by the cavity radius, whereas the period only influences the spectral position of the diffraction limit (i.e. the emissivity at shorter wavelengths). The increase of spectral efficiency with cavity height is decreasing and essentially negligible above a certain aspect ratio (diameter to height), the height of the cavity was thus limited to 8.0 μm. in the optimization. The figure of merit used in the optimization was spectral selectivity η_{sp} defined as the ratio of the number of (useful) photons emitted in the desirable wavelength range given by the TPV cell to the overall emitted photons at a given operating temperature (Eq. 1). The parameters of the optimized designs for a target operating temperature of 1500K are given in Table 1.

Table 1: Parameters of optimized PhC designs.

Design	Cell	λ_{PV} (μm)	r(μm)	a(μm)	d(μm)
I	InGaAsSb	2.3	0.55	1.22	7.16
II	InGaAs	2.0	0.49	1.1	8.0
III	GaSb	1.8	0.43	0.96	8.0

2.2 Emitter spectral selectivity

To evaluate the performance of the selective emitters, the spectral selectivity and useful emitted power density are calculated as a function of operating temperature. The hemispherical emissivities of the optimized PhC are used. The useful wavelength range is given by the EQE of the PV cells. The spectral selectivity η_{sp} and the useful emitted power density P_{out} are defined as:

$$\eta_{sp} = \frac{\int_0^{\lambda_{PV}} \varepsilon(\lambda)\, e_b(\lambda)\, d\lambda}{\int_0^{\infty} \varepsilon(\lambda)\, e_b(\lambda)\, d\lambda} \tag{1}$$

$$P_{out} = \int_0^{\lambda_{PV}} \varepsilon(\lambda)\, e_b(\lambda)\, d\lambda \tag{2}$$

where $\varepsilon(\lambda)$ is the wavelength dependent emissivity of the emitter, $e_b = 2hc^2/[\lambda^5(e^{\frac{hc}{\lambda k_B T}} - 1)]$ is the Planck blackbody, λ is the wavelength, λ_{PV} is the target cutoff wavelength of the PV cell, h is Planck's constant, c is the speed of light, k_B is the Boltzmann constant, and T is the temperature.

The calculated spectral efficiency for two optimized PhC designs as a function of operating temperature is shown in Fig. 2b. At a target operating temperature of 1500K the spectral efficiency of PhC design I (InGaAsSb, $\lambda_{PV} = 2.3$ μm) is 57.0% and that of PhC design II (InGaAs, $\lambda_{PV} = 2.0$ μm) is 48.2%, increasing with temperature. The optimum operating temperature also depends on the PV cell, as the cell efficiency decreases with increasing incident irradiance at higher temperatures. In comparison, the spectral efficiency of flat Ta at a cutoff wavelength of 2.3 μm is 43.6% and 35.9% at 2.0 μm. In addition to increased selectivity, the useful emitted output power is much higher for the PhC emitter, as shown in Fig. 2a. At 1500K, the useful emitted irradiance below the cutoff wavelength is 6.9 W/cm^2 for the PhC emitter with an InGaAsSb PV cell, and 5.4 W/cm^2 with an InGaAs PV cell. In contrast, the useful emitted power using flat Ta is only 2.0 W/cm^2 and 1.7 W/cm^2 for a cutoff wavelength of 2.3 μm and 2.0 μm respectively. These results are summarized in Table 2. At this temperature, the spectral selectivity was found to increase by more than 10% using the selective emitter. Since the emissivity of the PhC approaches that of a blackbody for wavelengths $\lambda < \lambda_{cutoff}$ resulting in higher power density, the useful emitted irradiance was found to be selectively increased *by a factor of 3* using the selective emitter as compared to the non-structured surface.

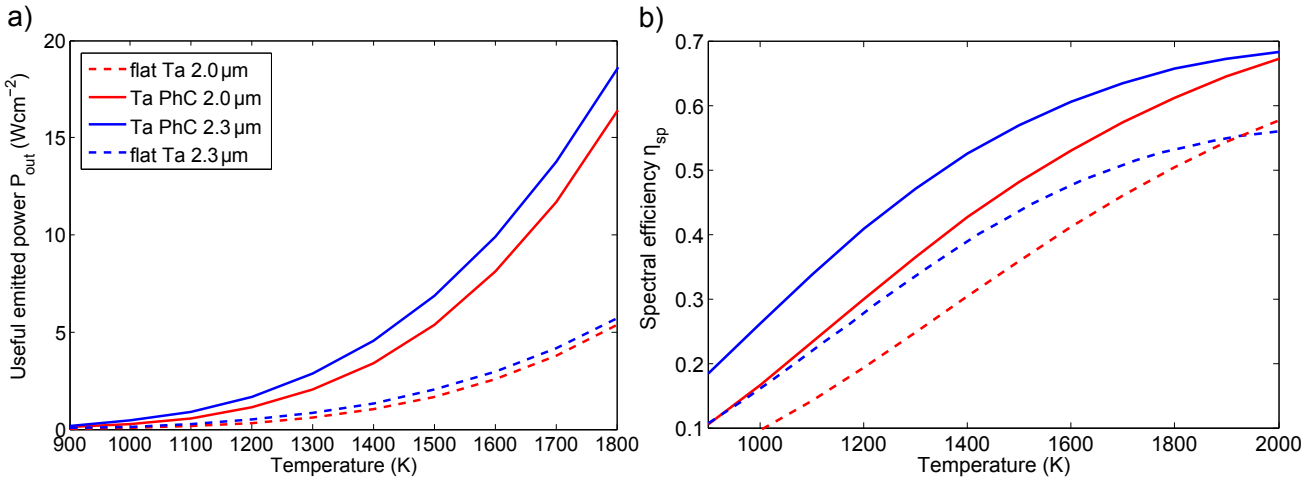

Figure 2: (Color online) (a) Useful emitted irradiance (power density P_{out}) and (b) spectral selectivity (η_{sp}) in dependence of the operating temperature for PhC design I (InGaAsSb, $\lambda_{PV} = 2.3\mu$m, blue) and II (InGaAs, $\lambda_{PV} = 2.0$ μm, red) and for flat Ta using the same cutoff wavelengths (dashed lines).

Table 2: Efficiency and power density comparison at 1500K.

Cell	Emitter	η_{sp} (%)	P_{out} (W/cm^2)
InGaAsSb	PhC I	57.0	6.9
InGaAsSb	Flat Ta	43.6	2.0
InGaAs	PhC II	48.2	5.4
InGaAs	Flat Ta	35.9	1.7

3. FABRICATION AND EXPERIMENTAL RESULTS

The substrates used in this study were prepared from an alloy of high purity polycrystalline Ta and W (2 - 3.5% concentration). The substrates were annealed in a Ta-lined high vacuum furnace at 1755°C for 8h under high vacuum to achieve thermal stability of the polycrystalline substrate material with large grain size. The substrates were cut, lapped to a thickness of 1 mm, and chemical-mechanically polished to achieve a roughness of less than 10 Å.

The fabrication of the PhCs, consisting of a square array of cylindrical cavities, is very similar to the one developed for Ta substrates[25] using interference lithography for large-area patterning. The cavity diameter is enlarged to the optimized value by isotropic plasma ashing and the pattern is subsequently transferred into a thin chrome (Cr) hard mask by reactive ion etching (RIE). For the final etching of the Ta substrate a Bosch etch process using SF_6 and C_4F_8 as the etching and passivating gaseous species was developed. It was observed that Ta 3% W can be etched in the same way as pure Ta. Up to 6 μm deep cavities in Ta with an aspect ratio (height to radius) of 6 to 1 were achieved by this fabrication process with very straight and smooth sidewalls. After removal of the chrome mask by wet etching, a thin film of HfO_2 (40 nm) was deposited on the etched Ta PhCs by ALD (Cambridge NanoTech Savannah), which facilitates conformal deposition even into the high-aspect ratio cavities. For the deposition of HfO_2 the substrate temperature was 250°C and (Tetrakis)dimethylmino Hafnium and water were used as precursors.

A PhC emitter with a measured cavity radius of $r = 0.53$ μm and a period $a = 1.3$ μm was fabricated, corresponding to PhC design I (InGaAsSb, $\lambda_{PV} = 2.3$ μm). The etch depth was experimentally measured by milling into the substrate using a focused ion beam (FIB) microscope and found to be $\sim 6\mu$m on average, corresponding to an aspect ratio of 6 to 1, as shown in Fig. 4a.

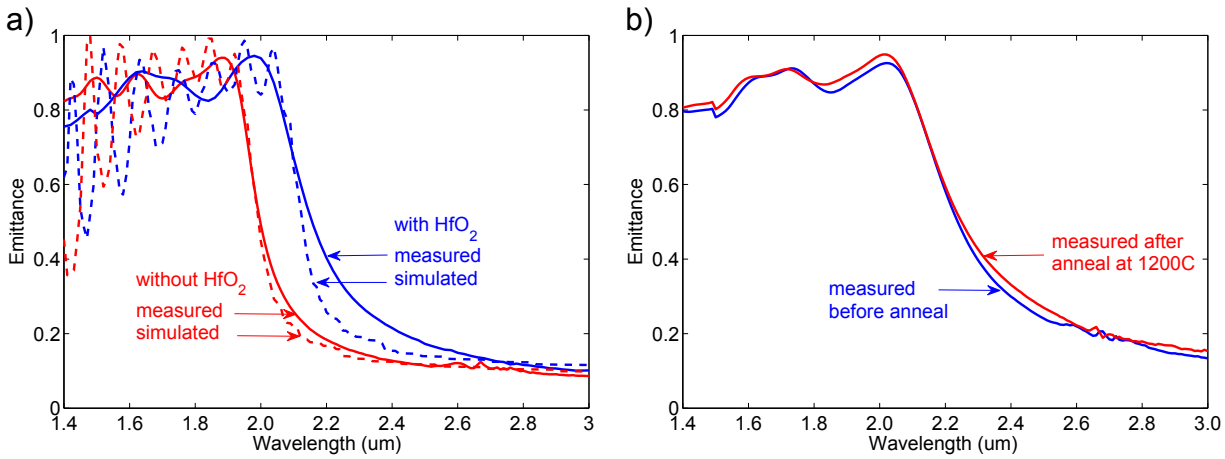

Figure 3: (Color online) (a) Comparison of the emittance obtained from reflectance measurements at room temperature of the Ta 3% W PhC without and with an HfO_2 coating of 40 nm thickness, and simulations using a period $a = 1.37$ μm, cavity depth $d = 6.7$ μm, and radius $r = 0.53$ μm and radius $r = 0.57$ μm respectively for the uncoated and coated PhC. (b) Comparison of the emittance of the Ta 3% W PhC with an HfO_2 coating before and after anneal at 1200°C for 24 h in a vacuum furnace with the emittance of the polished substrate.

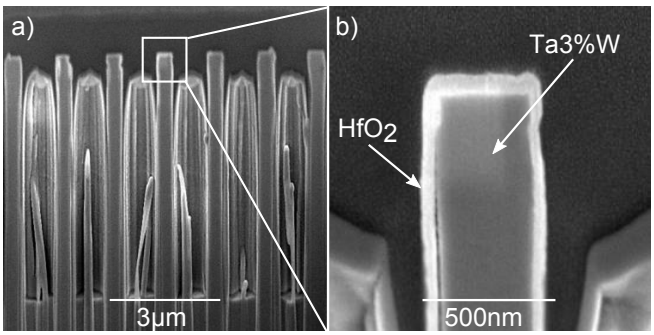

Figure 4: (a) FIB cross section of the Ta 3% W PhC after 24h anneal at 1200°C for 24 h in a vacuum furnace. Note that Pt was deposited prior to FIB milling in order to improve the cross-sectional imaging. (b) Close up of the cavity wall after anneal. No structural degradation is observed.

The emittance of the fabricated PhCs is obtained from near normal angle reflectance measurements at room temperature, using Kirchhoff's law by which the emittance $E = 1 - R$ for non-transmitting substrates. The numerical simulation using the previously measured cavity radius and period of the fabricated PhC ($r = 0.53$ μm and $a = 1.3$ μm) and a cavity depth of $d = 6.7$ μm shows good agreement to the emittance shown in Fig. 3a. The HfO_2 coating causes a slight shift of the cutoff wavelength, which can be taken into account in simulation and optimization of the PhC geometry. The fabricated emitters show high emittance below the cutoff wavelength while maintaining low emittance above, with a steep cutoff between. The spectral efficiency for the fabricated geometry is calculated from the simulated hemispherical data using high temperature material properties. Very good spectral selectivity is observed for the PhC emitters and the selectivity increases with temperature as expected. As discussed in Sect. 2.2, the total calculated hemispherical spectral efficiency is found to be greater than 50% above ~ 1200°C. System modeling shows that the expected TPV thermal-to-electrical efficiency using an InGaAsSb TPV cell and a matched PhC emitter (with no further spectral components such as filters) can reach 29.1% for ideal TPV cell properties, and 13.0% for actual measured TPV cell properties, both at an operating temperature of ~ 1200°C.[7]

To study the thermal stability, the fabricated PhCs were annealed at 1200°C for 24 h in a vacuum setup under Ar atmosphere (10^{-7} Torr base pressure, 10^{-4} Torr flowing UHP Ar) to prevent oxidation and degradation of the microstructured materials. The reflectance of the Ta 3% W PhCs with the HfO_2 ALD was coating obtained experimentally at room temperature before and after annealing by spectroradiometric measurement, as shown in Fig. 3b. The spectral emittance of the Ta 3% W PhC and its selectivity is essentially preserved after the 24h anneal at 1200°C. A small degradation of the cutoff tail is observed after anneal, as well as a slight increase of the emittance above the cutoff wavelength, which is attributed to carbide formation on the surface due to remaining carbon contamination in the vacuum system, as determined by Auger Electron Spectroscopy (AES). The structural stability of the Ta 3% W PhC with the HfO_2 ALD coating was studied through the FIB cross sectional images before and after annealing, showing no change of the PhC profile, as shown in Fig. 4b. Surface diffusion was effectively prevented by the HfO_2 coating at least for the observed time and temperature scale.

4. CONCLUSION

A 2D PhC was designed using FDTD numerical simulations and its spectral emittance was optimized to match a PV cell with a bandgap at 2.3 μm. The performance of different PhCs was also evaluated and compared to a system without a 2D PhC. At 1500K ($\sim$ 1200°C), the emitted irradiance (radiated power) in the useful wavelength range (given by the EQE of the PV cells) was found to be 6.9 W/cm^2 for the PhC emitter using an InGaAsSb PV cell, and 5.4 W/cm^2 using an InGaAs PV cell. In contrast, the useful radiated power was found to be only 2.0 W/cm^2 and 1.7 W/cm^2 using flat polished Ta as an emitter and a cutoff wavelength of 2.3 μm and 2.0 μm, respectively. The useful emitted irradiance is therefore selectively increased by a factor of 3 using the selective emitter compared to the non-structured surface. A PhC optimized for an InGaAsSb PV cell was fabricated on a Ta 3% W alloy substrate and a thin conformal coating of HfO_2 was used as a surface

protection and thermal barrier coating. The emittance of the Ta 3% W PhC was obtained from near-normal reflectance measurements at room temperature before and after annealing at 1200°C for 24 h in vacuum with a protective dielectric coating of 40 nm HfO_2, showing high spectral selectivity as predicted by simulations. A slight degradation of the emittance spectrum was attributed to the beginning of carbide formation on the surface of the HfO_2 coating (due to contamination), which is still greatly decelerated in contrast to the surface reaction on Ta without the coating. SEM images of the cross section of the PhC prepared by FIB milling compared before and after anneal confirm the structural stability of the HfO_2 coated Ta 3% W PhC and no degradation, i.e. rounding of the profile, was observed, which confirms that the coating effectively prevents structural degradation due to surface diffusion. All in all, this paper demonstrates the suitability of 2D PhCs fabricated on polycrystalline Ta 3% W substrates with an HfO_2 coating for high-temperature energy conversion.

ACKNOWLEDGMENTS

The authors would like to thank Bob Geil for DRIE at the Institute of Advanced Materials at the University of North Carolina, Paul Aimone from H.C. Starck for providing the Ta-W alloy substrates, James Daley at NSL at MIT for film deposition, and Tim Savas for assistance and training in IL. Fabrication of PhCs was done in part at the NSL at MIT and at CNS at Harvard University, a member of the National Nanotechnology Infrastructure Network (NNIN), which is supported by the National Science Foundation under NSF Award No. ECS-0335765. This work was partially supported by the Army Research Office through the ISN under Contract Nos. DAAD-19-02-D0002 and W911NF-07-D000. M.S. was partially supported by the MIT S3TEC Energy Research Frontier Center of the Department of Energy under Grant No. DE-SC0001299. V.R. was funded by the Austrian Science Fund (FWF): J3161-N20.

REFERENCES

[1] Doyle, E., Shukla, K., and Metcalfe, C., "Development and demonstration of a 25 watt thermophotovoltaic power source for a hybrid power system," Tech. Rep. TR04-2001, National Aeronautics and Space Administration (August 2001).

[2] Bitnar, B., Durisch, W., and Holzner, R., "Thermophotovoltaics on the move to applications," *Applied Energy* **105**(0), 430 – 438 (2013).

[3] Chan, W. R., Bermel, P., Pilawa-Podgurski, R. C. N., Marton, C. H., Jensen, K. F., Senkevich, J. J., Joannopoulos, J. D., Soljačić, M., and Celanovic, I., "Toward high-energy-density, high-efficiency, and moderate-temperature chip-scale thermophotovoltaics," *PNAS* **110**(14), 5309–5314 (2013).

[4] Chan, W. R., Wilhite, B. A., Senkevich, J. J., Soljacic, M., Joannopoulos, J., and Celanovic, I., "An all-metallic microburner for a millimeter-scale thermophotovoltaic generator," *Journal of Physics: Conference Series* **476**(1), 012017 (2013).

[5] Crowley, C. J., Elkouh, N. A., Murray, S., and Chubb, D. L., "Thermophotovoltaic Converter Performance for Radioisotope Power Systems," *AIP Conf. Proc.* **746**(1), 601–614 (2005).

[6] Lenert, A., Bierman, D. M., Nam, Y., Chan, W. R., Celanovic, I., Soljačić, M., and Wang, E. N., "A nanophotonic solar thermophotovoltaic device," *Nat Nano* **9**, 126–130 (2013).

[7] Yeng, Y. X., Chan, W. R., Rinnerbauer, V., Joannopoulos, J. D., Soljačić, M., and Celanovic, I., "Performance analysis of experimentally viable photonic crystal enhanced thermophotovoltaic systems," *Opt. Express* **21**, A1035–A1051 (Nov 2013).

[8] Andreev, V., Sorokina, S., Timoshina, N., Khvostikov, V., and Shvarts, M., "Solar cells based on gallium antimonide," *Semiconductors* **43**(5), 668–671 (2009).

[9] Wernsman, B., Siergiej, R., Link, S., Mahorter, R., Palmisiano, M., Wehrer, R., Schultz, R., Schmuck, G., Messham, R., Murray, S., Murray, C., Newman, F., Taylor, D., DePoy, D., and Rahmlow, T., "Greater than 20% radiant heat conversion efficiency of a thermophotovoltaic radiator/module system using reflective spectral control," *Electron Devices, IEEE Transactions on* **51**, 512–515 (March 2004).

[10] Dashiell, M., Beausang, J. F., Ehsani, H., Nichols, G. J., DePoy, D., Danielson, L., Talamo, P., Rahner, K., Brown, E., Burger, S., Fourspring, P., Topper, W., Baldasaro, P. F., Wang, C., Huang, R., Connors, M., Turner, G., Shellenbarger, Z., Taylor, G., Li, J., Martinelli, R., Donetski, D., Anikeev, S., Belenky, G., and Luryi, S., "Quaternary ingaassb thermophotovoltaic diodes," *Electron Devices, IEEE Transactions on* **53**, 2879–2891 (Dec 2006).

[11] Heinzel, A., Boerner, V., Gombert, A., Blsi, B., Wittwer, V., and Luther, J., "Radiation filters and emitters for the nir based on periodically structured metal surfaces," *J. Mod. Optic.* **47**(13), 2399–2419 (2000).

[12] Sai, H. and Yugami, H., "Thermophotovoltaic generation with selective radiators based on tungsten surface gratings," *Appl. Phys. Lett.* **85**(16), 3399–3401 (2004).

[13] Rephaeli, E. and Fan, S., "Tungsten black absorber for solar light with wide angular operation range," *Appl. Phys. Lett.* **92**(21), 211107 (2008).

[14] Celanovic, I., Jovanovic, N., and Kassakian, J., "Two-dimensional tungsten photonic crystals as selective thermal emitters," *Appl. Phys. Lett.* **92**(19), 193101 (2008).

[15] Araghchini, M., Yeng, Y. X., Jovanovic, N., Bermel, P., Kolodziejski, L. A., Soljačić, M., Celanovic, I., and Joannopoulos, J. D., "Fabrication of two-dimensional tungsten photonic crystals for high-temperature applications," *J. Vac. Sci. Technol. B* **29**(6), 061402 (2011).

[16] Arpin, K. A., Losego, M. D., and Braun, P. V., "Electrodeposited 3d tungsten photonic crystals with enhanced thermal stability," *Chem. of Mater.* **23**(21), 4783–4788 (2011).

[17] Nagpal, P., Josephson, D., Denny, N., DeWilde, J., Norris, D., and Stein, A., "Fabrication of carbon/refractory metal nanocomposites as thermally stable metallic photonic crystals," *J. Mater. Chem.* **21**, 10836–10843 (2011).

[18] Rinnerbauer, V., Yeng, Y. X., Chan, W. R., Senkevich, J. J., Joannopoulos, J. D., Soljačić, M., and Celanovic, I., "High-temperature stability and selective thermal emission of polycrystalline tantalum photonic crystals," *Opt. Express* **21**, 11482–11491 (May 2013).

[19] Stelmakh, V., Rinnerbauer, V., Geil, R. D., Aimone, P. R., Senkevich, J. J., Joannopoulos, J. D., Soljačić, M., and Celanovic, I., "High-temperature tantalum tungsten alloy photonic crystals: Stability, optical properties, and fabrication," *Applied Physics Letters* **103**(12), 123903 (2013).

[20] Sai, H., Kanamori, Y., and Yugami, H., "High-temperature resistive surface grating for spectral control of thermal radiation," *Appl. Phys. Lett.* **82**(11), 1685–1687 (2003).

[21] Schlemmer, C., Aschaber, J., Boerner, V., and Luther, J., "Thermal stability of microstructured selective tungsten emitters," *AIP Conference Proceedings* **653**(1) (2003).

[22] Oskooi, A. F., Roundy, D., Ibanescu, M., Bermel, P., Joannopoulos, J., and Johnson, S. G., "Meep: A flexible free-software package for electromagnetic simulations by the {FDTD} method," *Comput. Phys. Commun.* **181**(3), 687 – 702 (2010).

[23] Liu, V. and Fan, S., "{S4} : A free electromagnetic solver for layered periodic structures," *Computer Physics Communications* **183**(10), 2233 – 2244 (2012).

[24] Johnson, S. G., "The nlopt nonlinear-optimization package," (accessed April 7, 2014). `http://ab-initio.mit.edu/nlopt`.

[25] Rinnerbauer, V., Ndao, S., Xiang Yeng, Y., Senkevich, J. J., Jensen, K. F., Joannopoulos, J. D., Soljačić, M., Celanovic, I., and Geil, R. D., "Large-area fabrication of high aspect ratio tantalum photonic crystals for high-temperature selective emitters," *J. Vac. Sci. Technol. B* **31**(1), 011802 (2013).